ACS APPLIED MATERIALS & INTERFACES

Research Article

www.acsami.org

Monitoring Demineralization and Subsequent Remineralization of Human Teeth at the Dentin−Enamel Junction with Atomic Force Microscopy

Bob-Dan Lechner,*[,†] Stephanie Röper,[‡] Jens Messerschmidt,[§] Alfred Blume,[†] and Robert Magerle[‡]

[†]Institut für Chemie, Martin-Luther-Universität Halle-Wittenberg, Von-Danckelmann-Platz 4, 06120 Halle/Saale, Germany

[‡]Fakultät für Naturwissenschaften, Technische Universität Chemnitz, Reichenhainer Str. 70, 09107 Chemnitz, Germany

[§]Labor für Strukturanalyse Messerschmidt, Hallesche Str. 10, 06246 Bad Lauchstädt, Germany

Supporting Information

ABSTRACT: Using atomic force microscopy, we monitored the nanoscale surface morphology of human teeth at the dentin−enamel junction after performing successive demineralization steps with an acidic soft drink. Subsequently, we studied the remineralization process with a paste containing calcium and phosphate ions. Repeated atomic force microscopy imaging of the same sample areas on the sample allowed us to draw detailed conclusions regarding the specific mechanism of the demineralization process and the subsequent remineralization process. The about 1-μm-deep grooves that are caused by the demineralization process were preferentially filled with deposited nanoparticles, leading to smoother enamel and dentine surfaces after 90 min exposure to the remineralizing agent. The deposited material is found to homogeneously cover the enamel and dentine surfaces in the same manner. The temporal evolution of the surface roughness indicates that the remineralization caused by the repair paste proceeds in two distinct successive phases.

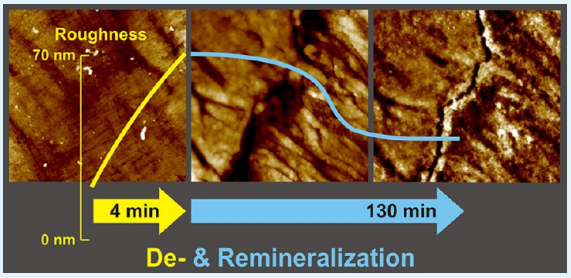

KEYWORDS: *tooth, dentine−enamel junction, remineralization, demineralization, erosion, GC Tooth Mousse, tapping mode atomic force microscopy*

INTRODUCTION

Dental erosion or demineralization (DEM) is the destruction of dental hard tissue triggered by acids from acidic food and beverages. Additionally, abrasions caused by mechanical impact can also cause material loss. Dental erosion in the form of enamel depletion is a possible initial step in caries formation: The resulting increase in roughness enables the acids produced by bacteria (mainly *Streptococcus mutans*, *lactobacilli*, and *actinomycetes*)[1−5] to more effectively attack the dental hard tissues. In contrast, remineralization (REM) is the formation of hydroxyapatite $Ca_5(PO_4)_3OH$ due to the precipitation and deposition of calcium phosphates from oversaturated calcium phosphate solutions or from protein complexes, such as caseinates from milk products or statherines[6] from native saliva. The proteins form soluble complexes with calcium phosphate nanoclusters, maintaining supersaturation and making these ions bioavailable. Therefore, the proteins act as transport vehicles supplying an ion reservoir.

The human tooth enamel is always exposed to a competition between DEM and REM. In the past 50 years, nutrition habits have changed and the DEM of enamel has become a serious problem.[7,8] Alimentation with mainly fast food or even with mainly fruit as well as the consumption of acidic or fruit drinks of natural origin cause a high degree of DEM.[9,10] Thus, it is necessary to find and study ways that REM can keep teeth healthy. The gingival recession and the erosion of enamel uncover the underlying dentine, which, in the majority of cases, is more vulnerable to attack from acids than enamel.[11] Therefore, we focused our research on the dentine−enamel junction (DEJ), because this region is the most vulnerable area on the tooth for demineralization processes.

There are a number of studies regarding the demineralization of dental hard tissue, dentine, and enamel, by acids and acidic drinks; these studies have shown that the tooth surface becomes rough as a result of minerals being leached out.[9,12−14] This process has been tracked by atomic force microscopy (AFM),[15] attenuated total reflection Fourier transform infrared spectroscopy (ATR-FTIR),[16] and nanoindentation experiments.[17−21] The effect of calcium-phosphate-loaded casein (calcium phosphopeptide-amorphous calcium phosphate, CPP-ACP complex) on affected tooth surfaces has also been studied.[20−24] The complex was shown to reduce the surface roughness of eroded dentine and enamel samples[25,26] and to reduce dentine hypersensitivities.[27−29] The application of the CPP-ACP complex combined with clinical tooth bleaching processes or the application together with self-

Received: October 5, 2014
Accepted: August 12, 2015

DOI: 10.1021/acsami.5b04790
ACS Appl. Mater. Interfaces XXXX, XXX, XXX−XXX

etching bonding agents resulted in less erosion of the enamel surfaces but also in reduced microshear bond strengths.[30] Furthermore, the paste is known to inhibit the growth of bacterial biofilms of *Streptococcus mutans* as well as fibroblasts on the tooth surface.[31,32]

AFM has been used to study the influence of different acids,[15,33] acidic soft drinks,[34] Tooth Mousse,[26,35] and other toothpaste formulations[36] on enamel and dentine surfaces. In these studies, a statistical analysis of the average roughness of polished tooth specimens was performed. For instance, Poggio et al.[25,26,35] reported that etching enamel first with an acidic soft drink and treating immediately afterward with a remineralizing paste caused a decrease in surface roughness compared to the roughness of samples that were only etched without any further treatment. With this methodology a remineralization effect on dentin was also reported for other toothpaste formulations.[36] Cheng and co-workers[12] proposed that etching the enamel produces a three-layer structure consisting of an outermost native layer which is completely removed by the acid, a softened layer in the middle, and a bottom transition layer which is not affected by the acid at all.

Here we monitor the nanoscale surface morphology at the dentin−enamel junction during demineralization with an acidic soft drink and subsequent remineralization with a repair paste. With tapping mode AFM (TM-AFM), we imaged the same area on the sample after successive de- and remineralization treatments. The study of the morphological changes at the dentin−enamel junction allows for a direct comparison of the behavior of these two different types of dental hard tissue. First, DEM was carried out by gradually treating polished human tooth slices with the acidic soft drink Coca-Cola. Then, REM was initiated by treating the specimens with a mixture of a paste containing calcium and phosphate ions (Tooth Mousse)[26] and saliva. Tooth Mousse paste is a water-based, sugar-free extraction from bovine milk and contains micellar calcium caseinate complexes made up of casein phosphopeptide (CCP) and amorphous calcium phosphate (ACP) nanoclusters.[9,24,37] Taking into account that the presence of saliva has a remarkable influence on the REM process due to its buffer properties and its natural content of calcium and phosphate ions,[38,39] the demineralized human tooth slices were treated with a mixture of Tooth Mousse paste and native saliva. For comparison, we also studied the mineralization effect on teeth treated only with native saliva.

MATERIALS AND METHODS

Sample Preparation. The human teeth used were caries-free adult incisors (collected at the dental practice Messerschmidt in Halle (Saale), Germany) from adult (30−60-year-old) female donors. After extraction, the teeth were mechanically cleaned and stored in bactericidal aqueous 0.5% Chloramine-T solution (Carl Roth GmbH & Co. KG, Karlsruhe, Germany) at 5 °C until being used within a few days. Since the tooth's exterior is corrugated and concave-curved at the native DEJ (position 2 in Figure 1a), this area is very difficult to access with the AFM tip. Therefore, we prepared thin slices and studied an artificial DEJ (position 1 in Figure 1a) which is not exposed to the oral cavity in vivo but is easily accessible with AFM. Before embedding the tooth in Technovit 3040 resin (Heraeus Kulzer GmbH, Wehrheim, Germany), the tooth was rinsed with water and immersed for 5 min in absolute ethanol (Carl Roth GmbH & Co. KG, Karlsruhe, Germany) to remove the aqueous solution from the tooth's exterior surface. After the resin hardened (2 h at ambient temperature), the tooth was sawed with a Minitom precision cutoff machine (Struers GmbH, Willich, Germany) parallel to the tooth longitudinal axis within the sagittal plane of the tooth to produce slices with 1 mm thickness (Figure 1a).

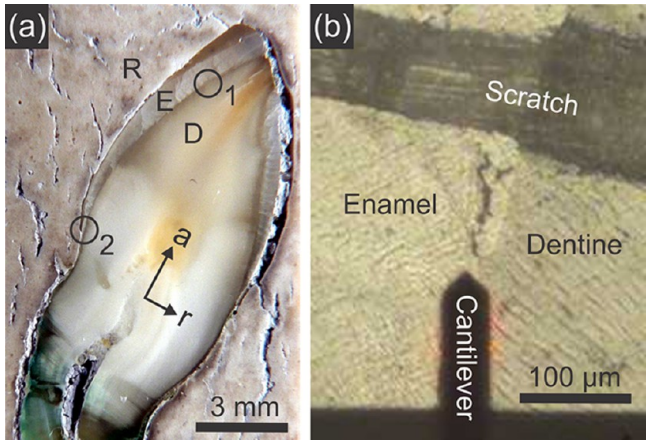

Figure 1. (a) Optical micrograph of a tooth slice with cut direction along the tooth longitudinal axis *a* in the sagittal plane. The enamel (E), the dentine (D), and the resin (R) are clearly distinguishable. Position 1 was studied with AFM; the native enamel−dentine junction is at position 2. (b) Optical micrograph of the AFM tip at the dentine−enamel junction at the position 1. The anticipated longitudinally oriented dentine tubules appear as dark stripes in the dentine region.

The sawing direction was chosen so as to avoid uncovering the dentine tubules. Open dentine tubules often lead to artifacts in the AFM images due to the enormous height differences the AFM tip has to overcome. A scalpel was used to apply an artificial scratch to the tooth slices next to the region of interest and almost perpendicular to the DEJ (Figure 1b). The scratch, the dentin enamel interface, and polishing marks allow the AFM tip to be repositioned to the same area of interest after each treatment step. To produce flat surfaces, the tooth slices were mechanically ground using Microsent silicon carbide abrasive papers (with a granularity from P1200 to P4000; Buehler GmbH, Düsseldorf, Germany) under water irrigation. For surface finishing, the samples were polished with a suspension of diamond particles 1 μm in diameter (Buehler GmbH, Düsseldorf, Germany).

De- and Remineralization Procedures. For DEM, the human tooth slices were etched in vitro with fresh, well carbonated Coca-Cola (20 mL, pH = 2.42 measured at 20 °C) for 30 s. The etching solution was kept at room temperature and was not stirred. Subsequently, the specimens were rinsed with distilled water and immediately dried in an air stream. For every sample, the etching and drying procedure was repeated nine times and AFM measurements were carried out after each step. The total soft-drink application time (4.5 min) was specifically chosen as a range of time likely to reflect a person's possible daily ingestion of soft drinks. The amount of soft drink at each etching step and the application time (30 s) mimic a few sips.

After this demineralization procedure, the tooth slices were treated in vitro with a mixture of 3 mg of Tooth Mousse paste (GC, Tokyo, Japan) and ca. 5 mL of native saliva. The saliva was taken from one person after thorough teeth brushing and intensive irrigation with water, followed by a waiting time of 5 min. The remineralization process was conducted seven times for each sample with a 10 min incubation time, which corresponds to the recommended application time of the Tooth Mousse paste. After the seven REM steps, we added two treatments with a 30 min incubation time. After each treatment, the paste residues were removed by rinsing with water, and the slices were air-dried and then imaged with AFM.

With a control group of specimens, we investigated the REM activity of pure salvia. Four tooth slices from two caries-free adult incisors were first etched stepwise with the acidic soft drink as described before and then treated in vitro only with saliva (5 mL) in steps of 10 and 30 min as described above. The DEJ at position 1 (Figure 1a) was imaged with AFM after each treatment step.

More than 20 tooth slices from 6 different teeth were investigated within this study. Excessive drying of the tooth samples was prevented

DOI: 10.1021/acsami.5b04790
ACS Appl. Mater. Interfaces XXXX, XXX, XXX−XXX

by storing them in bactericidal aqueous solution and preventing long periods (>60 min) without water contact during the measurements. All the treatment steps and imaging were performed at room temperature.

Imaging with AFM. The investigations were carried out with a MultiMode atomic force microscope with a Nanoscope IV controller (Digital Instruments, Santa Barbara, CA) coupled with a reflected-light microscope (Olympus MM10, Olympus Europa Holding GmbH, Hamburg, Germany). A scratch and characteristic features on the sample surface were used to reposition the AFM tip to the same area of interest after each processing step (Figure 1b). The specimen samples were measured in air in tapping mode (TM-AFM) using NCH-type silicon cantilevers (NanoWorld, Neuchâtel, Switzerland) with nominal tip radii smaller than 10 nm and a spring constant of 42 N/m. The AFM images were recorded over an area of 40 μm × 40 μm in the region of the tooth crown at the lingual or vestibular DEJ (position 1 in Figure 1a) with an acquisition speed of 12 μm/s (0.15 Hz line rate) and a lateral resolution of 512 pixels × 512 pixels. A first-order plane was fitted to the AFM height images and subtracted to correct for sample tilt. For the animated sequence of AFM height images, the images were registered by a rigid body transformation, using the tool StackReg[40] in the image software Fiji.[41]

RESULTS

Figure 2 shows a series of TM-AFM height images of a polished tooth slice after stepwise demineralization with the acidic soft drink Coca-Cola. The first image (Figure 2a) shows the ground and polished tooth surface without chemical treatment. The dashed yellow line indicates the interface between enamel (upper-left) and dentine (lower-right). The numbered white labels mark characteristic positions on the sample. The criss-cross structure (indicated by blue arrows) are marks caused by the mechanical polishing. Figure 2b–e shows the effect of the etching process. With increasing DEM time, the roughness of the surface increases (see the yellow ellipses in Figure 2a and e) and ridges and grooves appear at the enamel and the dentine side of the specimen. Due to this increase in roughness, the *z*-scale (height) of the last two images (Figure 2d and e) was adjusted from 1 to 2 μm. It should be noted that the most remarkable changes happen at the interface region between the dentine and the enamel (Figure 2e, dashed yellow line).

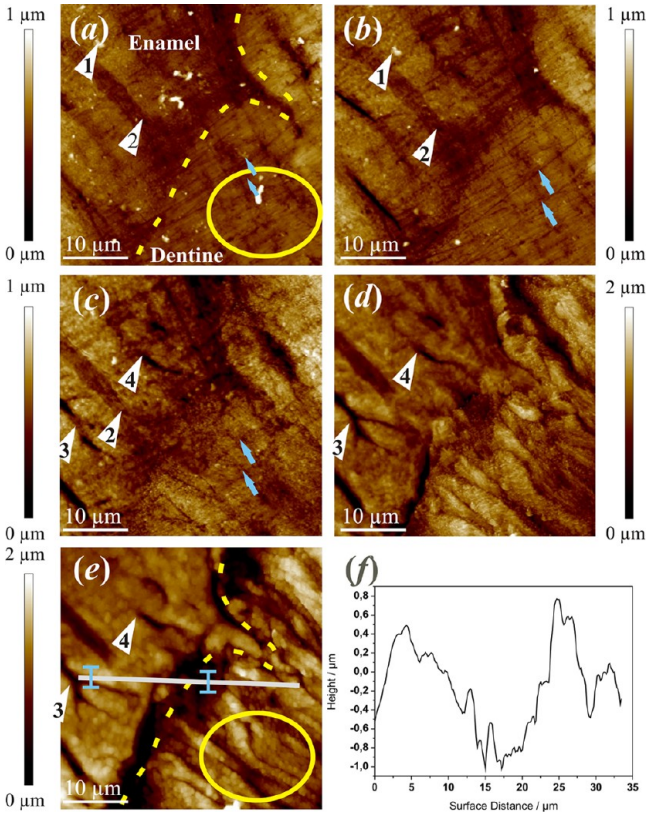

Figure 2. TM-AFM height images of the junction between the dentine (right) and enamel (left) after treatment with the acidic soft drink. (a) After mechanical grinding; after (b) 30 s, (c) 90 s, (d) 180 s, and (e) 240 s exposure to the acidic soft drink. Panels (a–e) show the same region on the specimen as indicated by characteristic positions (white arrows) and polishing marks (blue arrows). The yellow dashed lines indicate the junction between the dentine and enamel. (f) Height profile extracted along the white line shown in (e).

To follow the changes within the interface region in more detail, the surface roughness and the maximal depth of the interface cleft, obtained from cross section measurements, are plotted versus the DEM time t_{DEM} in Figure 3. Cross sections were taken of each image, spanning the interfacial region as indicated in Figure 2e and f. The maximal depth of the interfacial cleft increases with the DEM time from 200 nm initially up to 400 nm after t_{DEM} = 3 min. The process becomes much more pronounced for t_{DEM} > 3 min, and the depth increases to 1.4 μm (Figure 3b). Additionally, the root-mean-square (RMS) roughness was measured in three 5 μm × 5 μm large areas within the 40 μm × 40 μm large AFM images, excluding the deep cleft at the DEJ. The average RMS roughness is plotted as a function of the DEM time (Figure 3a) with error bars indicating the standard deviation. The RMS roughness increases continuously with DEM time. This increase is also reflected by the increase in the standard deviation.

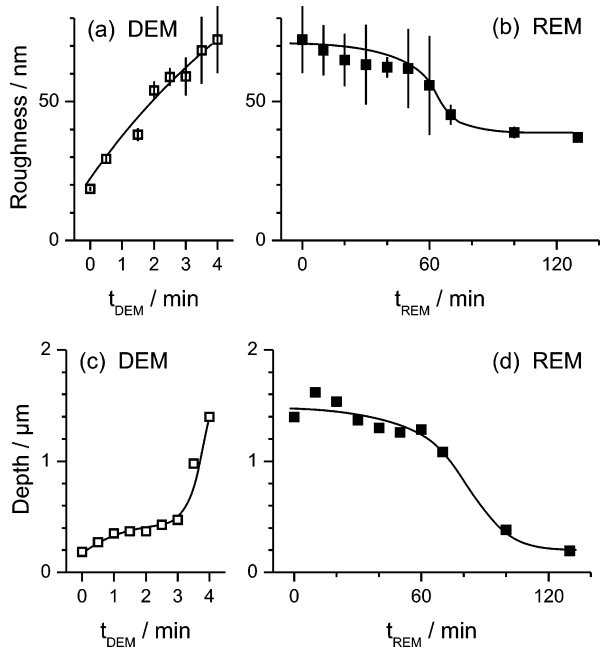

Figure 3. RMS roughness (a, b) and maximal depth of the cleft at the dentine–enamel junction (c, d) as determined from cross section measurements at the position indicated in Figure 2e as a function of DEM time (a, c) and REM time (b, d); the lines are guides to the eye.

Subsequently, the remineralization was carried out by applying a mixture of Tooth Mousse paste and native saliva

DOI: 10.1021/acsami.5b04790
ACS Appl. Mater. Interfaces XXXX, XXX, XXX–XXX

to the same (maximally demineralized) sample. The numbered white triangles in Figure 4 indicate identical positions on the

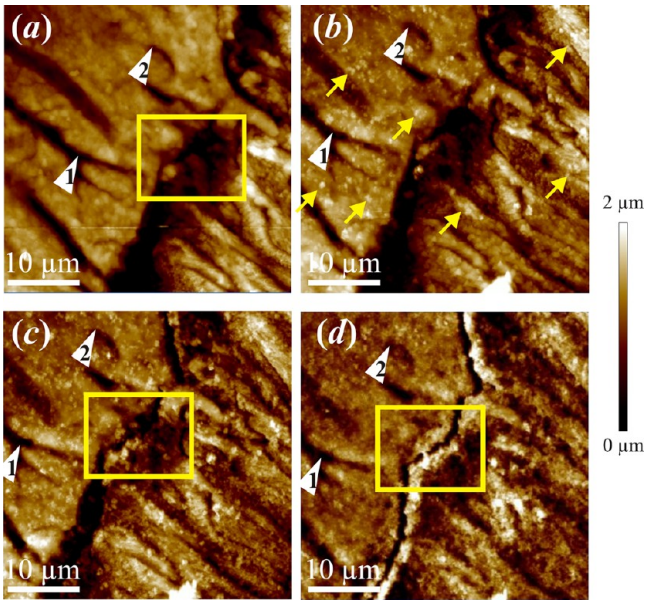

Figure 4. TM-AFM height images of the dentine (right) and enamel (left) after gradually etching with the acidic soft drink for a total of 240 s and REM with a mixture of Tooth Mousse and native saliva for 10 min (a), 40 min (b), 70 min (c), and 130 min (d). White markers show characteristic positions; yellow arrows mark deposited artificial enamel nanoparticles; yellow rectangles emphasize the cleft at the dentine–enamel junction.

sample surface. After 20 min of REM (Figure 4b), it is obvious that nanoparticles have been deposited on the surfaces of both the dentine and enamel (yellow arrows). Such particles are not only deposited on the flat areas but also in the deep cleft, which is notable at the dentin-enamel junction (yellow rectangle, Figure 4a, c, and d). Moreover, after 130 min of treatment with the Tooth Mousse and saliva mixture, the cleft at the dentin–enamel junction is refilled almost completely, resulting in a smoother surface with a smaller RMS roughness (40 nm) and only a small groove between the enamel and dentine (Figure 4d).

For the REM process, the depth of the cleft and the RMS surface roughness have been determined and plotted versus the REM time t_{REM} (Figure 3b, d). Both the RMS roughness and the depth of the cleft decrease with increasing REM time with a considerable decrease after 60 min REM time. This indicates that the temporal evolution of the remineralization of the dentine and enamel surface as well as the filling of the interface cleft is characterized by two distinct successive phases.

Figure 5 shows the TM-AFM height and phase contrast images of another de- and remineralization experiment performed in the same way as described previously. On the left side of the images, the enamel face can be seen, and on the right side, the dentine. The yellow dashed line indicates the interface between the two areas. After mechanical polishing (Figure 5a, d), the difference between the enamel and dentine regions in terms of the tip–sample interaction at the surface is small, as indicated by the phase contrast (Figure 5d). We note that many factors contribute to the phase contrast, like viscoelastic surface properties, adhesion forces, and local roughness. Due to the grinding process, there is an all-over covering with ablated enamel, dentine, and material from the resin matrix (Technovit 3040). Upon etching, the native tooth structures are uncovered (Figure 5b), and the different surface properties of dentine and enamel are clearly visible in the phase images (Figure 5e). After 240 s of etching followed by 130 min of remineralization, no differences between the enamel and dentine region are distinguishable in the phase-contrast image (Figure 5f), indicating that the same material is deposited on the two different surfaces.

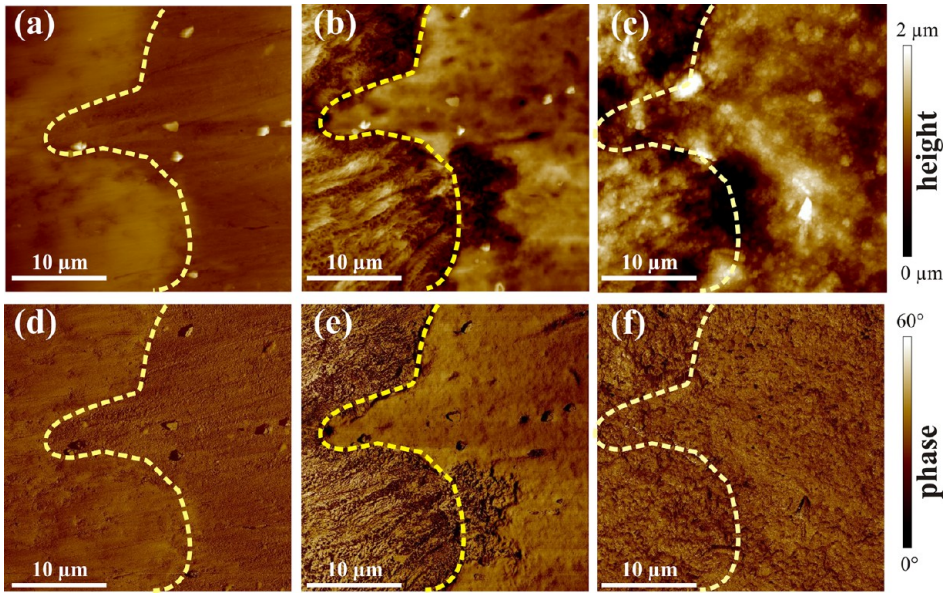

Figure 5. TM-AFM height (a–c) and phase (d–f) images of the dentine (right) and enamel (left) after grinding and polishing (a, d), after etching with the acidic soft drink for 240 s (b, e), and after REM with a mixture of Tooth Mousse and native saliva for 70 min (c, f). The dashed line marks the dentine–enamel junction. An animated sequence of all the AFM height images taken after successive de- and remineralization steps is shown in the Supporting Information.

DOI: 10.1021/acsami.5b04790
ACS Appl. Mater. Interfaces XXXX, XXX, XXX–XXX

For comparison, we also studied the impact of pure saliva on the REM process. Tooth slices were first gradually eroded with the acidic soft drink and then treated with pure saliva under the in vitro conditions described previously (Figure 6). Even after

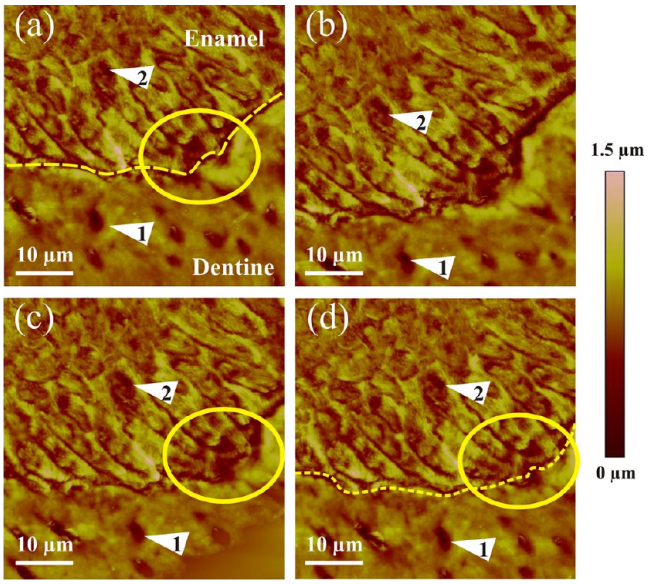

Figure 6. TM-AFM height images of the dentine (bottom) and enamel (top) after gradually etching with the acidic soft drink for a total of 240 s (a) and after treatment with native saliva for 20 min (b), 60 min (c), and 190 min (d). White markers show characteristic positions; the yellow ellipse marks a sector of the dentine–enamel junction region.

very long treatment times (190 min, Figure 6d), no detectable degree of REM is seen. This result shows that the REM effect caused by the mixture of saliva and the tooth repair paste is mainly caused by the repair paste containing calcium and phosphate ions.

DISCUSSION

In the present study, we used the tapping mode AFM technique to study the nanoscale erosion processes induced by an acidic soft drink on human tooth enamel and dentine at the dentine–enamel junction as well as to study the subsequent remineralization process and the effect of exposing both dental hard tissues to either a mixture of Tooth Mousse paste and saliva (experimental group) or just native saliva (control group). The application times were chosen to mimic a typical consumption pattern of an acidic soft drink and the recommended repeated application of remineralization pastes. At room temperature, the etching rate of dentine and enamel is ~20% smaller than that at 37 °C,[42] the crystallization rate of hydroxyapatite is 2/3 of that at 37 °C,[43] and the enamel remineralization rate is 1/3 of that at 37 °C,[44] but the general processes are qualitatively the same as those at 37 °C. The key distinguishing characteristic of our study is that we could image the same position at the dentin–enamel junction during DEM and REM, thus revealing detailed information on the nanometer scale regarding the changes as they occurred over time. In particular, we were able to observe the local change of the nanoscale surface morphology and roughness.

The progressive impact of an acidic drink on the teeth leads to considerable depletion of the material on the dentine and on the enamel surfaces (Figure 2). Treatment with the acidic soft drink for 30 s, which is comparable to a few sips, already led to an observable degradation of the tooth surfaces (Figure 2b). After further treatment with the acidic soft drink, the deep criss-cross structure, which originated from the grinding process, vanishes and the natural surface morphology of the material becomes apparent (Figure 2c, d). Enamel prisms are oriented oblique to the imaging plane and are therefore not visible. During the entire etching process, the roughness of the surface increases. For total DEM times shorter than 180 s, we observe a moderate increase in surface roughness with respect to increasing DEM time, whereas for total DEM times longer than 180 s, a significant increase in roughness can be seen. Possibly, during the first 180 s of total DEM time, the erosion process involves the softening of the dental materials; after this time, the process just involves the removal of plain material. The loss of material from the dentine region is significantly larger than from the enamel region, since dentine is somewhat softer than enamel and has a lower mineral content and higher protein (collagen) content. However, the most remarkable erosion occurs at the interface region between both materials (at the dentin–enamel junction), where a cleft is formed. With progressing DEM time, this interface cleft becomes deeper (Figure 3c). We expect that this demineralization process is typical in the case of a soft drink containing phosphoric acid. The formation of trenches in both enamel and dentine and the formation of a cleft at the DEJ resemble the morphology formed during intergranular corrosion. Recent work on rodent enamel shows that the increased solubility of grain boundaries during acid etching is due to their amorphous structure and different chemical compostion.[42]

REM occurs much more slowly than DEM, and therefore, longer treatment times were chosen (10 and 30 min). After 10 min of treatment with the remineralizing agent, there is no visible change in the surface topography (Figure 4a). During further REM, material in the form of globular particles (presumably hydroxyapatite or inorganic calcium phosphate)[45] is observed to refill the grooves (Figure 4b–d). This smoothening is also reflected in the decrease of the RMS roughness and the decrease of the depth of the cleft at the dentin–enamel junction (Figure 3c, d).

Figure 7 shows a model for the DEM and REM processes on enamel and dentine. The model is partly based on the model

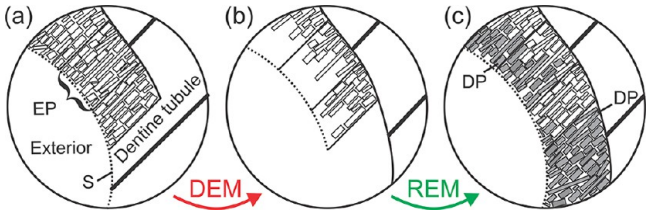

Figure 7. Schematic representation of the de- and remineralization processes. (a) Native enamel and dentine surface, (b) mineral loss after treatment with acidic drinks and alteration of the tooth surface S, and (c) mineral deposition during REM. EP is an enamel prism, and DP is the deposited particle material.

proposed in refs 46 and 47. It illustrates the structural change of dental hard tissue surfaces (position S, in Figure 7a), the process of mineral loss (Figure 7b), and the deposition of material (Figure 7c) in the form of small deposited particles (DP) growing within the native enamel prisms (EP, black bars). Particles are also deposited upon the eroded dentine surface.

DOI: 10.1021/acsami.5b04790
ACS Appl. Mater. Interfaces XXXX, XXX, XXX–XXX

We observe that the deposition of material on etched dentine surfaces occurs in the same way as on enamel surfaces. Thus, the new material is deposited on native enamel, on native dentine, as well as on the interface region, resulting a homogeneous covering. We expect the deposited inorganic particles to be calcium phosphate. In the process, the particles' morphology and orientation depends on several aspects, like the viscosity of the REM agents, local variations of the chemical composition, and the local interaction pattern with the protein casein.[48−50]

In the AFM phase images, we can distinguish between the enamel and dentine by a slight difference in the phase shift values measured on the polished sample (Figure 5d); this difference becomes even more evident after the sample is treated with the acidic soft drink (Figure 5e). After REM, the enamel and dentine regions can hardly be distinguished in the AFM phase image (Figure 5f). From this, we conclude that the same material is deposited on both the dentine and enamel surfaces, resulting in a homogeneous covering of both surfaces. Therefore, REM techniques like the one used in this study might be suitable for covering free-standing dentine areas which are present due to gingival regression or local plenary enamel depletion. Also, it might be possible to cover exposed dentine tubule apertures to achieve an analgesic effect. Such an effect has been reported for polished dentine specimens.[36]

When we compare the surface roughness after 240 s of etching to the surface roughness after 130 min of REM (Figure 3b), it is clear that the REM process does not lead to the same smooth surface as obtained by polishing. This indicates that the in vitro experiments performed here are still different than the in vivo situation. In the latter case, the REM process induced by saliva will probably be present immediately after the DEM process. The surface roughness of the tooth will also depend on the individual tooth care measures used by the individual, which determine the presence or absence of bacterial biofilms.

With REM under the applied conditions, it takes about 2 h to completely cover the eroded surface. This suggests that the thickness of the deposited layer in an in vivo application is probably much smaller, as the usual application time of Tooth Mousse paste is only about 20 min. However, in everyday life, the demineralization will probably be less severe compared to the demineralization resulting from the conditions used in our study, because remineralization will also occur due to the presence of saliva with its natural content of calcium and phosphate ions during the intermittent consumption of acidic drinks and food. Furthermore, natural saliva acts as a buffer and thus reduces the acidic erosion at the tooth surface. Saliva seems to play a crucial role for the formation and precipitation of enamel.[38] Thus, there might be an additional REM contribution of saliva in between the Tooth Mousse applications irrespective of the paste's impact in vivo.

SUMMARY

We monitored the nanoscale surface morphology at the dentine−enamel junction upon exposure to an acidic soft drink and during the subsequent remineralization process with a mixture of saliva and a paste containing calcium and phosphate ions. Our experiments model the de- and remineralization process of teeth occurring in everyday life. Successive AFM imaging reveals how the dentine−enamel junction is gradually eroded over time and an about 1-μm-deep cleft is formed. The subsequent exposure of the specimen to the remineralization agent leads to the deposition of mineral nanoparticles, homogeneously covering both enamel and dentine, in a similar manner. The temporal evolution of the surface roughness shows that the remineralization process occurs much more slowly than previously expected and that it proceeds in two distinct successive phases.

ASSOCIATED CONTENT

Supporting Information

The Supporting Information is available free of charge on the ACS Publications website at DOI: 10.1021/acsami.5b04790.

Animated sequence of AFM height images taken after successive de- and remineralization steps. Three images from this sequence are shown in Figure 5 (AVI)

AUTHOR INFORMATION

Corresponding Author

*E-mail: bob-dan.lechner@chemie.uni-halle.de.

Notes

The authors declare no competing financial interest.

ACKNOWLEDGMENTS

The acquisition of the AFM was supported by the Volkswagen Foundation and the Deutsche Forschungsgemeinschaft. We thank C. Vetter for help with the sample preparation, S. Kubitza for help with the AFM measurements, the dental patients for donating their extracted teeth, D. Voigt for discussions, and M. Neumann for compiling the animated sequence of AFM images.

REFERENCES

(1) Hamada, S.; Slade, H. D. Biology, Immunology, and Cariogenicity of Streptococcus Mutans. *Microbiol. Rev.* **1980**, *44*, 331−384.

(2) Crossner, C.-G. Salivary Lactobacillus Counts in the Prediction of Caries Activity. *Community Dent. Oral Epidemiol.* **1981**, *9*, 182−190.

(3) Ellen, R. P.; Banting, D. W.; Fillery, E. D. Streptococcus Mutans and Lactobacillus Detection in the Assessment of Dental Root Surface Caries Risk. *J. Dent. Res.* **1985**, *64*, 1245−1249.

(4) Tanzer, J.; Livingston, J.; Thompson, A. The Microbiology of Primary Dental Caries in Humans. *J. Dent. Educ.* **2001**, *65*, 1028−1037.

(5) Filoche, S. K.; Anderson, S. A.; Sissons, C. H. Biofilm Growth of Lactobacillus Species Is Promoted by Actinomyces Species and Streptococcus Mutans. *Oral Microbiol. Immunol.* **2004**, *19*, 322−326.

(6) Masica, D. L.; Gray, J. J. Solution- and Adsorbed-State Structural Ensembles Predicted for the Statherin-Hydroxyapatite System. *Biophys. J.* **2009**, *96*, 3082−3091.

(7) Lussi, A.; Hellwig, E.; Ganss, C.; Jaeggi, T. Buonocore Memorial Lecture: Dental Erosion. *Oper. Dent.* **2009**, *34*, 251−262.

(8) Lussi, A. *Dental Erosion: From Diagnosis to Therapy*; Karger; Basel, 2006; Vol. *20*.

(9) Marshall, G. W.; Wu-Magidi, I. C.; Watanabe, L. G.; Inai, N.; Balooch, M.; Kinney, J. H.; Marshall, S. J. Effect of Citric Acid Concentration on Dentin Demineralization, Dehydration, and Rehydration: Atomic Force Microscopy Study. *J. Biomed. Mater. Res.* **1998**, *42*, 500−507.

(10) Lippert, F.; Parker, D. M.; Jandt, K. D. Toothbrush Abrasion of Surface Softened Enamel Studied with Tapping Mode AFM and AFM Nanoindentation. *Caries Res.* **2004**, *38*, 464−472.

(11) West, N. X.; Hughes, J. A.; Addy, M. Erosion of Dentine and Enamel in Vitro by Dietary Acids: The Effect of Temperature, Acid Character, Concentration and Exposure Time. *J. Oral Rehabil.* **2000**, *27*, 875−880.

(12) Cheng, Z.-J.; Wang, X.-M.; Cui, F.-Z.; Ge, J.; Yan, J.-X. The Enamel Softening and Loss During Early Erosion Studied by Afm, Sem and Nanoindentation. *Biomed. Mater.* **2009**, *4*, 015020.

DOI: 10.1021/acsami.5b04790
ACS Appl. Mater. Interfaces XXXX, XXX, XXX−XXX

(13) Barbour, M. E.; Rees, J. S. The Laboratory Assessment of Enamel Erosion: A Review. *J. Dent.* **2004**, *32*, 591−602.
(14) Cheng, L.; Li, J. Y.; Huang, S.; Zhou, X. D. Effect of Galla Chinensis on Enhancing Remineralization of Enamel Crystals. *Biomed. Mater.* **2009**, *4*, 034103.
(15) Quartarone, E.; Mustarelli, P.; Poggio, C.; Lombardini, M. Surface Kinetic Roughening Caused by Dental Erosion: An Atomic Force Microscopy Study. *J. Appl. Phys.* **2008**, *103*, 104702−104706.
(16) Wang, X.; Klocke, A.; Mihailova, B.; Tosheva, L.; Bismayer, U. New Insights into Structural Alteration of Enamel Apatite Induced by Citric Acid and Sodium Fluoride Solutions. *J. Phys. Chem. B* **2008**, *112*, 8840−8848.
(17) Barbour, M. E.; Parker, D. M.; Jandt, K. D. Enamel Dissolution as a Function of Solution Degree of Saturation with Respect to Hydroxyapatite: A Nanoindentation Study. *J. Colloid Interface Sci.* **2003**, *265*, 9−14.
(18) Lippert, F.; Parker, D. M.; Jandt, K. D. In Vitro Demineralization/Remineralization Cycles at Human Tooth Enamel Surfaces Investigated by Afm and Nanoindentation. *J. Colloid Interface Sci.* **2004**, *280*, 442−448.
(19) Barbour, M. E.; Shellis, R. P. An Investigation Using Atomic Force Microscopy Nanoindentation of Dental Enamel Demineralization as a Function of Undissociated Acid Concentration and Differential Buffer Capacity. *Phys. Med. Biol.* **2007**, *52*, 899.
(20) White, A. J.; Gracia, L. H.; Barbour, M. E. Inhibition of Dental Erosion by Casein and Casein-Derived Proteins. *Caries Res.* **2011**, *45*, 13−20.
(21) Abdullah, A. Z.; Ireland, A. J.; Sandy, J. R.; Barbour, M. E. A Nanomechanical Investigation of Three Putative Anti-Erosion Agents: Remineralisation and Protection against Demineralisation. *Int. J. Dent.* **2012**, *2012*, 76812.
(22) Reynolds, E. C. Anticariogenic Complexes of Amorphous Calcium Phosphate Stabilized by Casein Phosphopeptides: A Review. *Special Care in Dentistry* **1998**, *18*, 8−16.
(23) Cochrane, N. J.; Saranathan, S.; Cai, F.; Cross, K. J.; Reynolds, E. C. Enamel Subsurface Lesion Remineralisation with Casein Phosphopeptide Stabilised Solutions of Calcium, Phosphate and Fluoride. *Caries Res.* **2008**, *42*, 88−97.
(24) Kumar, V. L. N.; Itthagarun, A.; King, N. M. The Effect of Casein Phosphopeptide-Amorphous Calcium Phosphate on Remineralization of Artificial Caries-Like Lesions: An in Vitro Study. *Aust. Dent. J.* **2008**, *53*, 34−40.
(25) Poggio, C.; Lombardini, M.; Colombo, M.; Bianchi, S. Impact of Two Toothpastes on Repairing Enamel Erosion Produced by a Soft Drink: An AFM in Vitro Study. *J. Dent.* **2010**, *38*, 868−874.
(26) Poggio, C.; Lombardini, M.; Dagna, A.; Chiesa, M.; Bianchi, S. Protective Effect on Enamel Demineralization of a Cpp-Acp Paste: An AFM in Vitro Study. *J. Dent.* **2009**, *37*, 949−954.
(27) Piekarz, C.; Ranjitkar, S.; Hunt, D.; McIntyre, J. An in Vitro Assessment of the Role of Tooth Mousse in Preventing Wine Erosion. *Aust. Dent. J.* **2008**, *53*, 22−25.
(28) Manton, D. J.; Bhide, R.; Hopcraft, M. S.; Reynolds, E. C. Effect of Ozone and Tooth Moussetm on the Efficacy of Peroxide Bleaching. *Aust. Dent. J.* **2008**, *53*, 128−132.
(29) Jorgensen, M. G.; Carroll, W. B. Incidence of Tooth Sensitivity after Home Whitening Treatment. *J. Am. Dent. Assoc., JADA* **2002**, *133*, 1076−1082.
(30) Adebayo, O. A.; Burrow, M. F.; Tyas, M. J. Dentine Bonding after Cpp-Acp Paste Treatment with and without Conditioning. *J. Dent.* **2008**, *36*, 1013−1024.
(31) Rahiotis, C.; Vougiouklakis, G.; Eliades, G. Characterization of Oral Films Formed in the Presence of a Cpp-Acp Agent: An in Situ Study. *J. Dent.* **2008**, *36*, 272−280.
(32) Cehreli, S. B.; Gurpinar, A. O.; Onur, A. M.; Dagli, F. T. In Vitro Evaluation of Casein Phosphopeptide-Amorphous Calcium Phosphate as a Potential Tooth Transport Medium: Viability and Apoptosis in L929 Fibroblasts. *Dent. Traumatol.* **2008**, *24*, 314−319.
(33) Watari, F. In Situ Quantitative Analysis of Etching Process of Human Teeth by Atomic Force Microscopy. *J. Electron Microsc.* **2005**, *54*, 299−308.
(34) Finke, M.; Parker, D. M.; Jandt, K. D. Influence of Soft Drinks on the Thickness and Morphology of in Situ Acquired Pellicle Layer on Enamel. *J. Colloid Interface Sci.* **2002**, *251*, 263−270.
(35) Poggio, C.; Lombardini, M.; Vigorelli, P.; Ceci, M. Analysis of Dentin/Enamel Remineralization by a Cpp-Acp Paste: Afm and Sem Study. *Scanning* **2013**, *35*, 366−374.
(36) Poggio, C.; Lombardini, M.; Vigorelli, P.; Colombo, M.; Chiesa, M. The Role of Different Toothpastes on Preventing Dentin Erosion: An SEM and AFM Study. *Scanning* **2014**, *36*, 301−310.
(37) Horne, D. S. Casein Micelle Structure: Models and Muddles. *Curr. Opin. Colloid Interface Sci.* **2006**, *11*, 148−153.
(38) Klimek, J.; Hellwig, E.; Ahrens, G. Fluoride Taken up by Plaque, by the Underlying Enamel and by Clean Enamel from Three Fluoride Compounds in Vitro. *Caries Res.* **1982**, *16*, 156−161.
(39) Dawes, C. What Is the Critical pH and Why Does a Tooth Dissolve in Acid? *J. Can. Dent. Assoc.* **2003**, *69*, 722−725.
(40) Thevenaz, P.; Ruttimann, U. E.; Unser, M. A Pyramid Approach to Subpixel Registration Based on Intensity. *IEEE Trans. Image Process* **1998**, *7*, 27−41.
(41) Schindelin, J.; Arganda-Carreras, I.; Frise, E.; Kaynig, V.; Longair, M.; Pietzsch, T.; Preibisch, S.; Rueden, C.; Saalfeld, S.; Schmid, B.; Tinevez, J.-Y.; White, D. J.; Hartenstein, V.; Eliceiri, K.; Tomancak, P.; Cardona, A. Fiji: An Open-Source Platform for Biological-Image Analysis. *Nat. Methods* **2012**, *9*, 676−682.
(42) Gordon, L. M.; Cohen, M. J.; MacRenaris, K. W.; Pasteris, J. D.; Seda, T.; Joester, D. Amorphous Intergranular Phases Control the Properties of Rodent Tooth Enamel. *Science* **2015**, *347*, 746−750.
(43) Meyer, J. L.; Nancollas, G. H. The Effect of pH and Temperature on the Crystal Growth of Hydroxyapatite. *Arch. Oral Biol.* **1972**, *17*, 1623−1627.
(44) Arends, J.; Ten Cate, J. M. Tooth Enamel Remineralization. *J. Cryst. Growth* **1981**, *53*, 135−147.
(45) ten Cate, J. M.; Arends, J. Remmeralization of Artificial Enamel Lesions in Vitro. *Caries Res.* **1977**, *11*, 277−286.
(46) Gelhard, T. B. F. M. Dissertation, University of Groningen, 1982.
(47) Arends, J.; Gelhard, T. B. F. M. Die Schmelz-Remineralisation in Vivo. *Colloquium Med. Dent.* **1983**, *27*, 295−304.
(48) Li, L.; Pan, H.; Tao, J.; Xu, X.; Mao, C.; Gu, X.; Tang, R. Repair of Enamel by Using Hydroxyapatite Nanoparticles as the Building Blocks. *J. Mater. Chem.* **2008**, *18*, 4079−4084.
(49) Fowler, C. E.; Li, M.; Mann, S.; Margolis, H. C. Influence of Surfactant Assembly on the Formation of Calcium Phosphate Materials-a Model for Dental Enamel Formation. *J. Mater. Chem.* **2005**, *15*, 3317−3325.
(50) Robinson, C.; Connell, S.; Kirkham, J.; Shore, R.; Smith, A. Dental Enamel-a Biological Ceramic: Regular Substructures in Enamel Hydroxyapatite Crystals Revealed by Atomic Force Microscopy. *J. Mater. Chem.* **2004**, *14*, 2242−2248.

DOI: 10.1021/acsami.5b04790
ACS Appl. Mater. Interfaces XXXX, XXX, XXX−XXX